

# Application of microCT scanning in the recovery of endo-skarn associated scheelite from the Riviera Deposit, South Africa

Abraham Rozendaal<sup>a,\*</sup>, Stephan G. Le Roux<sup>b</sup>, Anton du Plessis<sup>b</sup>

<sup>a</sup> Department of Earth Sciences, University of Stellenbosch, South Africa

<sup>b</sup> CAF X-ray Facility University of Stellenbosch, South Africa

## ARTICLE INFO

**Keywords:**  
Scheelite  
Beneficiation  
MicroCT

## ABSTRACT

The granite-hosted Riviera W-Mo-REE deposit is an approximately 40 million ton low grade (~0.2% WO<sub>3</sub>) endo-skarn resource and contains disseminated scheelite as the principle ore. Scheelite is strongly zoned and has a molybdenum-rich core and depleted rim. Separation of the high-demand low-molybdenum scheelite does not appear possible. The high density contrast between scheelite ( $\rho = 6.1$ ) and gangue ( $\rho = 2.7$ ) allows separation by gravity on tables, wet or dry spirals and heavy medium liquids. In the present laboratory study the latter method was used as a pre-concentration stage and yielded at best a ~50% scheelite recovery of the -1 mm size fraction. The generally fine grain size of the liberated grains and considerable loss to the -45  $\mu\text{m}$  fraction is a function of the friable nature of scheelite and possible overgrinding. The influence of this mineralogical characteristic on scheelite recovery will have to be accommodated in the beneficiation in particular the comminution stage, of the deposit in the future. As a complimentary study MicroCT scanning was applied as a relatively new analytical tool to evaluate the beneficiation results obtained. The method studied both sinks and floats of the various size fractions and allowed quantification of scheelite grain size distribution and calculation of ore grade of the coarse fractions. MicroCT images displayed the textural relationships between the ore and gangue minerals and the degree of scheelite liberation. This analytical tool proved useful in the present study and the results indicate that it can be applied to similar ore beneficiation studies.

## 1. Introduction

The Riviera W-Mo-REE deposit is located in the Piketberg area of the Western Cape Province and is hosted by late stage granites of the Neoproterozoic-Cambrian Cape Granite Suite (Rozendaal et al., 1994, 1999). The tabular-shaped ore body has an unclassified mineral resource of 46 million tons @ 0.216% WO<sub>3</sub>, 0.025% Mo using a 15 m thickness cutoff and extending to a vertical depth below surface of 220 m. Within this ore body, a high grade portion was delineated with unclassified mineral resources of: 7 million tons @ 0.279% WO<sub>3</sub>, 0.02% Mo. Rare earth element concentration in the deposit is highly anomalous, but resources have not been calculated. The style of mineralization is that of an endoskarn closely associated with pervasively hydrothermally altered, early quartz monzonite porphyry (QMP), biotite monzogranite (BMG) and late-stage aphanitic granite-monzogranite (AGM), (Rozendaal and Scheepers, 1995; Rozendaal and Boshoff, 2011; Rozendaal and Theart, 2013). Scheelite (CaWO<sub>4</sub>) is the only tungsten-bearing mineral and molybdenite (MoS<sub>2</sub>) reflects the molybdenum

grade. Rare earth elements are mainly hosted by allanite a member of the epidote group.

Scheelite is most abundant in the zones of endoskarn and the bordering skarnified granite. Together they define a favourable zone present as a cupola in the roof of the Riviera pluton (Fig. 1). Although abundant quartz veins traverse the Riviera pluton not all of them contain scheelite. Grain size of scheelite is highly variable but generally medium- to coarse-grained (50–600  $\mu\text{m}$ ) and shape anhedral to euhedral. It has two distinct and one less prominent cleavage direction and as a result is friable despite a Moh hardness of 4.5–5. Specific gravity of scheelite varies between 5.9 and 6.1.

All the scheelite grains observed display strong zonal crystal growth, the result of variation in crystal chemistry (Fig. 2). In general two distinct generations of scheelite have been identified. The yellow fluorescent-type with high molybdenum (1000–4000 ppm) is the earlier phase and shows overgrowths of late stage blue fluorescent scheelite which is relatively depleted in molybdenum (1–100 ppm; Pieterse et al., 2014).

\* Corresponding author.

E-mail address: [ar@sun.ac.za](mailto:ar@sun.ac.za) (A. Rozendaal).

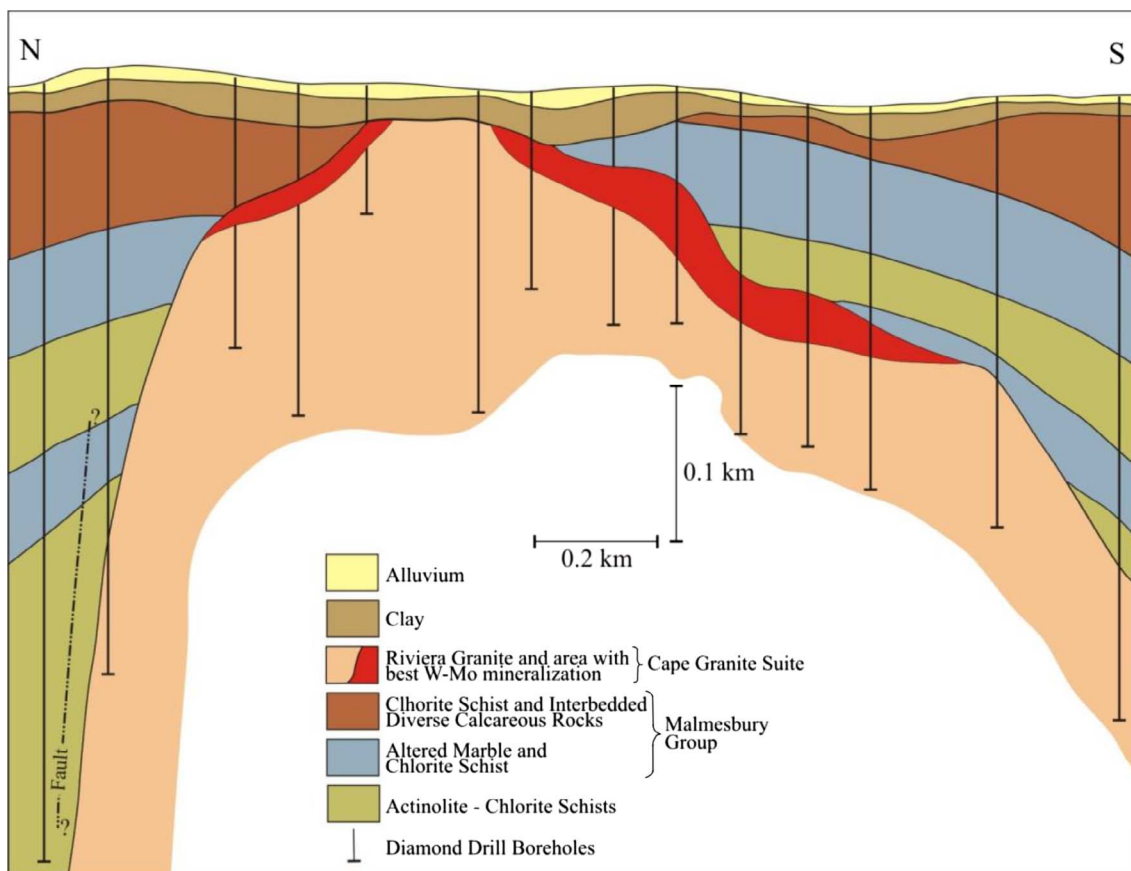


Fig. 1. Schematic vertical cross-section of the Riviera pluton showing the W-Mo-REE mineralized zone located on the contact between the granite host and Malmesbury Group meta-volcanosedimentary wall rocks.

2. Aims

The specific gravity of scheelite varies between 5.9 and 6.1 and contrasts sharply with the gangue mineralogy which consists of quartz, feldspar and hydrated alteration products ( $\rho < 2.9$ ) as well as the silicate mineralogy of the skarn zones (garnet  $\rho \sim 4.0$ , clinopyroxene  $\rho = 3.5\text{--}4.0$ , titanite, zoisite and epidote). Ore minerals are present in minor to trace concentrations and consist of pyrite, pyrrhotite, molybdenite, allanite, chalcopyrite and sphalerite ( $\rho = 4\text{--}4.5$ ). This density contrast between ore and gangue minerals allows the separation and beneficiation of these phases by gravity either on tables, wet or dry spirals or by means of high density liquids. As a result it was suggested

that scheelite beneficiation of the Riviera deposit should be considered by means of conventional heavy medium separation as a pre-concentration stage. This report presents the results of an orientation study that used split core from a diamond drill hole that intersected a representative mineralized section of the Riviera ore zone. As a second aim of the project the microCT scanner was introduced to test its application and capabilities as an additional/alternative analytical tool in the minerals industry and beneficiation of granite-hosted scheelite in particular. The use of microCT in the geosciences is growing steadily and has been reviewed recently by Cnudde and Boone (2013). The general use of microCT for analysis of ore minerals including particle size analysis was discussed in Kyle and Ketcham (2015). The use of

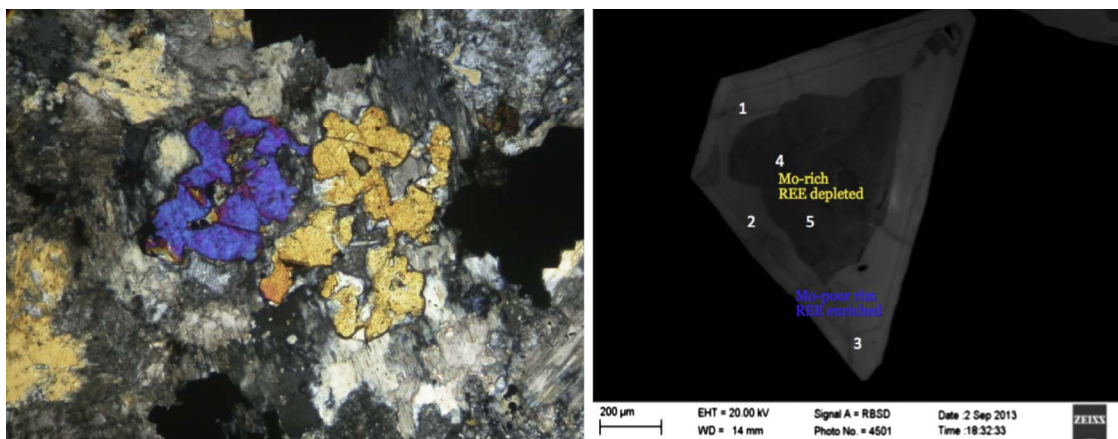


Fig. 2. a) Anhedra scheelite hosted by hydrothermally altered monzogranite indicated by sericitization of the feldspars (XPL). b) Scanning electron microscope image of euhedral scheelite showing oscillatory zoning with a molybdenum-rich core and depleted rim.

microCT as analytical tool applied to ore deposits was also discussed in a recent review by Pearce et al. (2017). Particle size analysis was also demonstrated previously in a study of phosphate rock flotation grade/recovery by Miller et al. (2009). The microCT aspect of this study was to demonstrate its ease of use and limited sample preparation and how the method can be applied with respect to texture imaging, grain size distribution and ore grade determination in the beneficiation process. One of the major drawbacks of microCT in the minerals industry is the lack of knowledge of its accuracy and the paper attempts to answer some these questions within the context of minerals processing of scheelite ore.

The novelty of microCT demonstrated here lies in the application and interpretation of the segmentation method which has a direct influence on the accuracy of the method.

### 3. Methodology

The sample selected for this exercise was derived from borehole BB/CC +350 which forms part of a selection of 112 diamond drill holes completed by Anglo American Corporation in the late 1970's early 1980's. The entire ore zone as defined by a 0.1% WO<sub>3</sub> cut-off was sampled between depths of 154–184 m. This 30 m length of quartered NQ/BX core had a mass of 35.63 kg and grade of 0.207% WO<sub>3</sub>. The average grade was obtained from a previous exercise that split and resampled a number of the old AAC boreholes in 2012–2013 (Fig. 3; Rozendaal and Theart, 2013). Intertek-Genalysis from Australia was responsible for the assaying using CRM standards and JORC compliant procedures.

The borehole is considered representative of the Riviera deposit as it has a thickness similar to the average thickness (31 m) and grade (0.214% WO<sub>3</sub>) as defined by Walker (1994) and Rozendaal and Theart (2013). The high grade (~0.3% WO<sub>3</sub>) section of the deposit was not considered for this exercise.

### 3.1. Sample preparation

The 35.63 kg bulk sample was crushed using a Wedag jaw crusher to 100% -20 mm. The sample was then split into four equal ~9 kg fractions by means of a Wedag riffler splitter. These fractions were then crushed to a 100% pass -10 mm, -4.75 mm (reported as -5 mm), -2 mm and -1 mm respectively using a Wedag disk mill and SABS (South African Bureau of Standards) approved test screens/sieves. This equipment is located at the Central Analytical Facility (CAF), University of Stellenbosch.

### 3.2. Heavy medium separation

The heavy medium separation was outsourced and conducted by Scientific Services of Cape Town. The following procedure was followed:

- Samples were sorted, dried and dried weights recorded.
- De-sliming was done at 45 μm and involves passing the entire sample through the selected screen after attritioning for 5 min.
- The +45 μm material is dried and weighed with the loss recorded as % slimes.
- The heavy mineral fraction is removed from the dried +45 μm fraction using TBE (tetra-bromo-ethane) which has a specific gravity (SG) of 2.95. The THM (total heavy mineral) fraction (sinks) is recorded as a percentage of the total mass. The fraction with an SG of < 2.95 is recorded as floats.
- In total three fractions are produced slimes, floats and sinks (THM) for chemical analyses.
- Percentage recovery per fraction is calculated as a function of WO<sub>3</sub> mass in sink and WO<sub>3</sub> mass in initial sample.

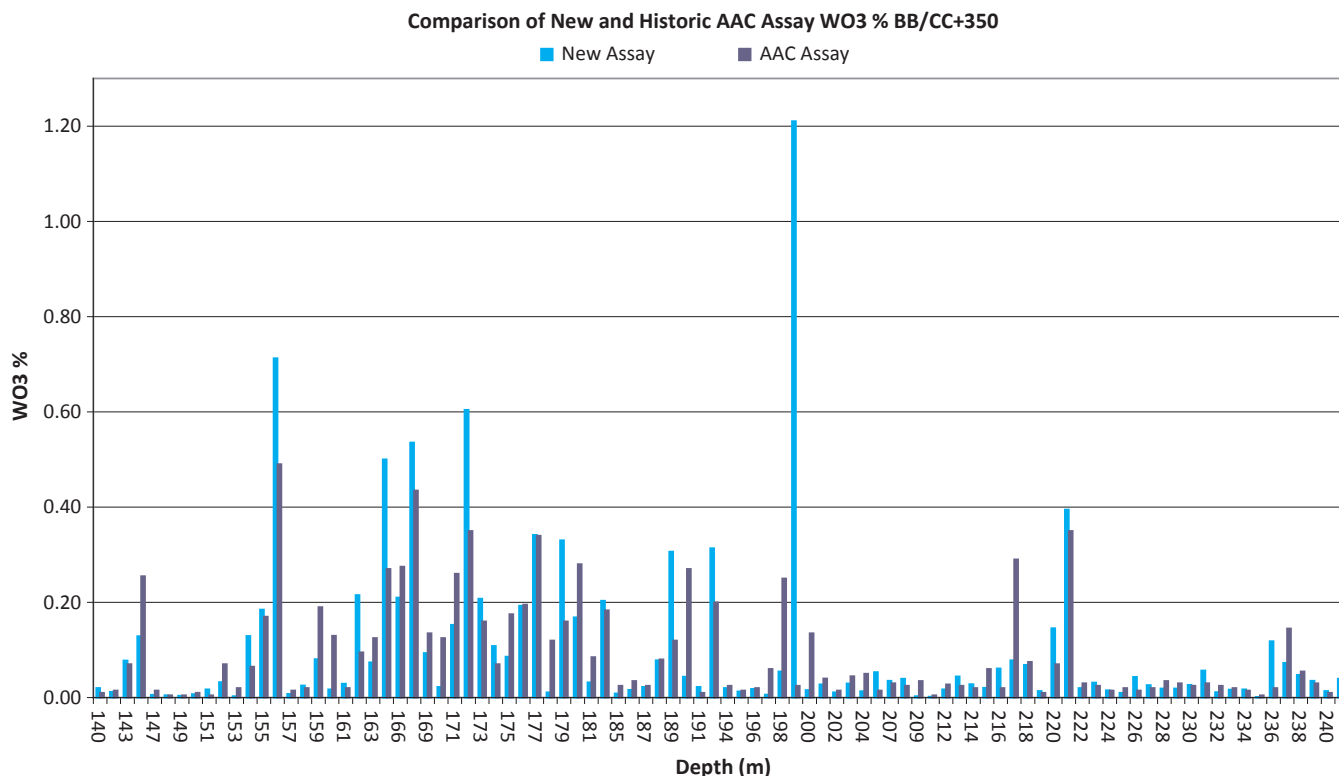


Fig. 3. Histogram showing down-the-hole variation of WO<sub>3</sub> grade of borehole BB/CC + 350. The ore intersection selected for this study has a grade of 0.207% WO<sub>3</sub> over a total length of 30 m and is located between 154 and 184 m. The result of sampling in the 1970's showed a slightly lower grade of 0.19% WO<sub>3</sub> over the same 30 m interval.

### 3.3. Chemical analyses

The three fractions obtained i.e. slimes, floats and sinks (THM) were analysed by Scientific Services of Cape Town using conventional XRF (X-ray fluorescence using CRM standards and a detection limit of 5 ppm) on pressed pellets. The results are reported as ppm  $\text{WO}_3$  and are the average of two iterations. This is a typical analysis for the minerals industry.

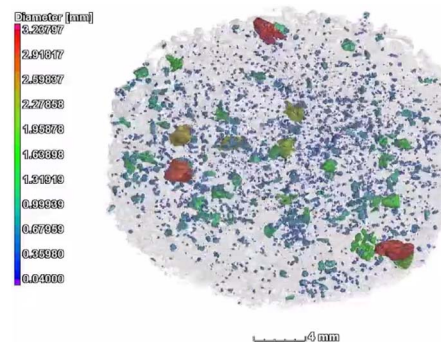
### 3.4. MicroCT

The sinks and floats of every size fraction were also studied by means of a high resolution microCT scanner. This allowed the identification, distribution characteristics and liberation of scheelite based on density contrasts. The scans were performed with a GE Phoenix v|tome|x at 200 kV, 100  $\mu\text{A}$  and a resolution of 20  $\mu\text{m}$  per voxel. The sample was loaded in a tube with a 25 mm diameter, and approximately 20 mm height. Scans included the use of a 0.5 mm copper filter to reduce beam hardening artefacts. All image analyses used Volume Graphics VGStudio Max 3.0 software. The facility is described in more detail in du Plessis et al. (2016).

The basic concepts of X-ray CT are briefly described as background information. An X-ray beam is generated with voltage and current settings adjustable to allow different penetrating energies (voltage) and beam intensity (current). The beam penetrates the sample, loaded between X-ray source and 2D detector. Due to different material absorptions (path lengths and X-ray absorption co-efficients – depending on atomic mass and physical density), different brightness values are recorded in the 2D X-ray image. By rotating the sample, images are recorded from many angles. By using these images, a 3D data set can be reconstructed using filtered back-projection of the 2D images. This 3D data set comprises of voxels (volumetric pixels) with brightest pixels corresponding to most dense material and dark pixels related to low density materials. Scanning parameters depend on sample type to be analysed and the type of analysis required. Various choices are made with regards to sample size, voxel size (resolution), number of images and image acquisition time, amongst others. A set of guidelines and principles was recently set out for biological specimens and the same principles generally apply to the geosciences (du Plessis et al., 2017). The parameters and optimum settings applied for the present study are a result of the application of the above-mentioned guidelines.

From the CT data, both the volumetric grade and the particle size distribution of the scheelite minerals were calculated. Initially, all scheelite in the samples needed to be segmented and digitally extracted using the segmentation method described by le Roux et al. (2015). This segmentation method involves the use of a global thresholding with a local optimization, which is a standard functionality of the software Volume Graphics VGStudioMax. This segmentation provided the bulk volume of the scheelite minerals, which could be used to calculate the total mass of scheelite using its known density. Since the entire scanned sample could be weighed, the volumetric grade could be determined as microCT scheelite mass/total mass. The same segmentation could be used to calculate the size and number of the individual grains, using the “Porosity/inclusion analysis” module of the software. The important aspect of this method for volumetric grade determination is the requirement that the entire sample fits in the field of view. This is achieved by loading the sample in a plastic tube with buffer foam above and below. This allows the width and height of the total sample to be roughly equal and entire scanned volume to be weighed. The microCT-derived volume and density of the scheelite was used in conjunction with the total sample weight to calculate the tungsten grade of each sample (le Roux et al., 2015). The measurement is thus dependant on total volume of scheelite determined by segmentation in microCT images. The segmentation and microCT image analysis is demonstrated in Fig. 4 using a sequence of images and described in more detail in Appendix 1. The calculated grade for sinks and floats of each size fraction was compared to the  $\text{WO}_3$  assay values determined by XRF

using industry-standard test methods and outsourced to a service provider for the minerals industry. MicroCT scans were repeated for 5 separate cuts from the same sample, for every size fraction of sinks and floats (40 scans in total). The results are summarized in Table 1. MicroCT scans of slimes were attempted but the grain sizes were too small to allow meaningful analytical results.



Video 1.

Volumetric grade determinations and grain size distributions of scheelite in both sinks and floats were calculated from the microCT data. The method did not allow the quantification of any parameters for the slimes fraction ( $-45 \mu\text{m}$ ) due to poor resolution relative to grain size of the slimes fractions (20  $\mu\text{m}$  voxel size at the  $20 \times 20 \times 20 \text{ mm}$  sample size used). Higher resolution is possible and might allow such quantification, but only for a much smaller sample size (e.g.  $2 \times 2 \times 2 \text{ mm}$  sample size for 2  $\mu\text{m}$  voxel size). This was not attempted due to the potential loss of representativity and practical reasons such as longer scan times. Development of methodology to quantify additional geometallurgical parameters such as scheelite liberation or percentage of scheelite locked with gangue, features that are clearly visible from the images generated, is planned for future work.

## 4. Results

### 4.1. De-sliming

De-sliming of the four size fractions showed an exponential increase in the percentage slimes generated with decreasing grain size (Table 2; Fig. 5). When crushing to  $-1 \text{ mm}$  for example, almost 19% of the mass is reduced to  $-45 \mu\text{m}$ . This size fraction is not conducive to the recovery of the high density minerals.

The slimes from all fractions contained a significant concentration of tungsten ranging between 0.19 and 0.25%  $\text{WO}_3$  (Table 3). The reduction in grain size is accompanied by an increased loss of tungsten oxide mass to the slimes fraction (Table 3; Fig. 6). The head grade used is 0.207%  $\text{WO}_3$  based on the average grade of the  $\sim 36 \text{ kg}$  sample (see Fig. 7).

### 4.2. Sinks and floats

The total heavy mineral concentration (THM or sinks) of each size fraction is presented in Table 4. The heavy mineral concentration increases systematically as the average grain size decreases, with maximum concentration in the  $-1 \text{ mm}$  fraction (Fig. 6). This indicates that liberation of the heavy minerals from the granitic matrix increases with grinding/milling to a finer grain size.

Although liberation increases linearly up to  $-2 \text{ mm}$  it flattens out slightly when grain size is further reduced and indicates that additional grinding to smaller grain size will not substantially increase liberation. The optimum liberation is probably achieved with milling to a 0.5–1 mm (500–1000  $\mu\text{m}$ ) grain size but this will have to be substantiated experimentally.

The  $\text{WO}_3$  grade of the slimes, sinks and floats of each size fraction as determined by XRF is presented in Table 5. The relationship between

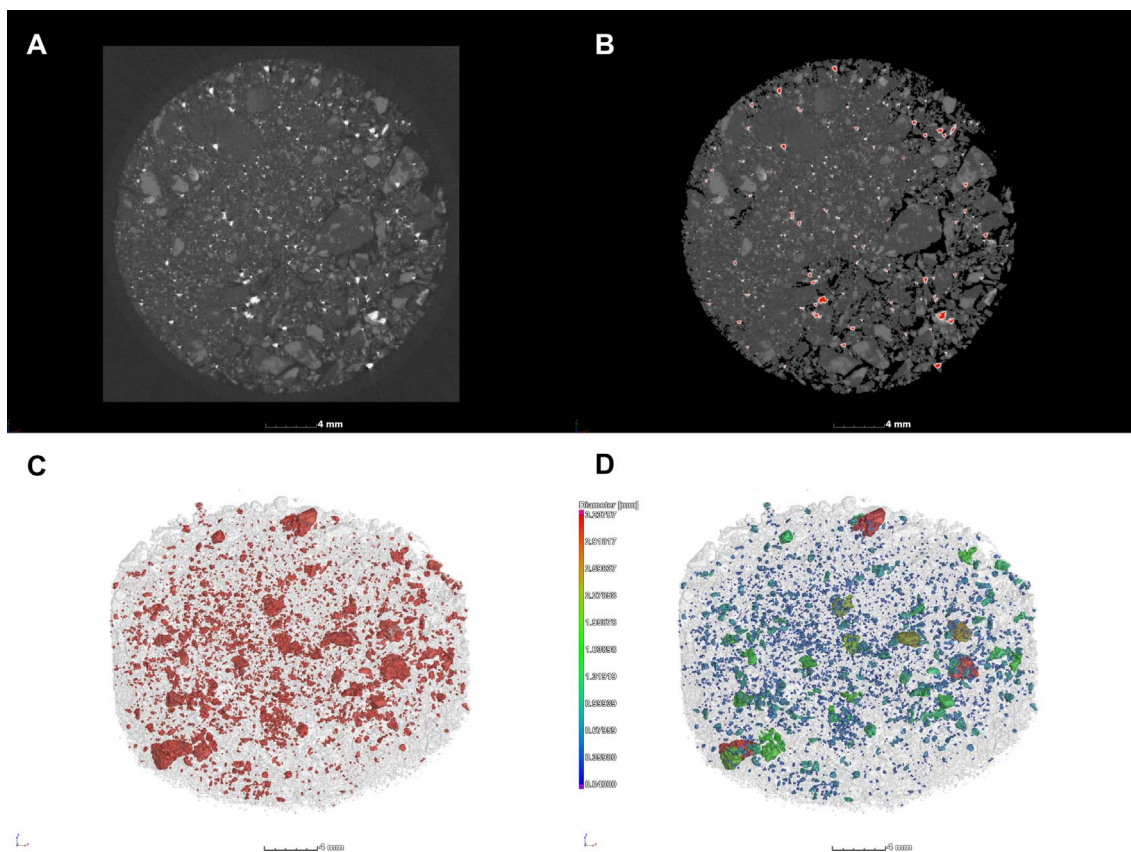


Fig. 4. Image segmentation and analysis of scheelite in sink – 5 mm sample: (a) raw microCT slice image, (b) segmented scheelite in pseudo-colour, (c) 3D rendering of scheelite grains (d) scheelite particle size analysis – colour coded by diameter. Video 1 available as supplementary material.

Table 1  
Summary of samples and WO<sub>3</sub> analyses.

	MicroCT, 20 μm	XRF assay
Floats – 10 mm	5 x	1 x
Floats – 5 mm	5 x	1 x
Floats – 2 mm	5 x	1 x
Floats – 1 mm	5 x	1 x
Sinks – 10 mm	5 x	1 x
Sinks – 5 mm	5 x	1 x
Sinks – 2 mm	5 x	1 x
Sinks – 1 mm	5 x	1 x
Slimes – 10 mm	No result	1 x
Slimes – 5 mm	No result	1 x
Slimes – 2 mm	No result	1 x
Slimes – 1 mm	No result	1 x

size fraction and sink WO<sub>3</sub> grade is graphically presented in Fig. 8.

The recovery of WO<sub>3</sub> as a percentage of the head grade increases with the reduction of grain size and attains a maximum of 47.9% for the – 1 mm size fraction (Table 6). Fig. 9 shows that there is limited increase in recovery when grain size is reduced from – 2 mm to – 1 mm.

Table 2  
Weight percent slimes (– 45 μm) generated per size fraction.

Sample Nr.	% Slimes
– 10 mm	4.18
– 5 mm	5.43
– 2 mm	11.78
– 1 mm	18.98

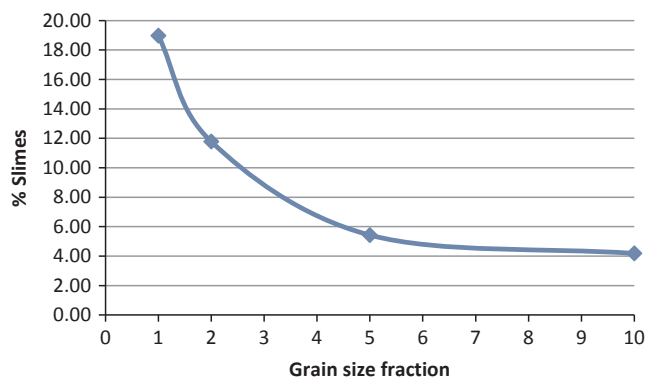


Fig. 5. Reduction in grain size is accompanied by considerable increase in the weight percent slimes generated. In this study slimes are defined as the – 45 μm fraction. Grain size fraction is in mm.

### 4.3. MicroCT

Floats, sinks (concentrates) and slimes of all four grain size fractions were subjected to microCT scanning. Settings were selected in order to analyse a representative volume of material in each scan i.e.

Table 3  
WO<sub>3</sub> mass loss in the slimes of each grain size fraction.

Sample Nr.	WO <sub>3</sub> kg/t% loss
– 10 mm	0.104/5.02
– 5 mm	0.127/6.14
– 2 mm	0.265/12.80
– 1 mm	0.360/17.39

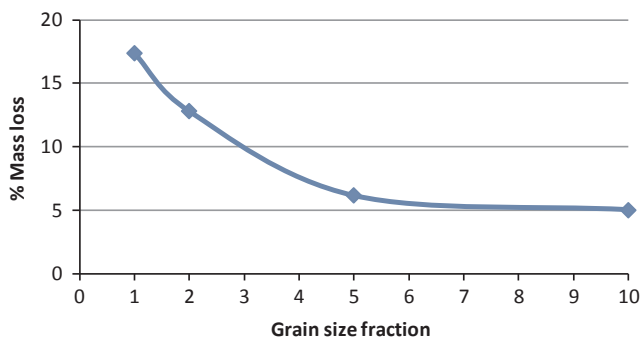


Fig. 6. Graph showing percentage WO<sub>3</sub> mass loss to slimes as a function of grain size fraction.

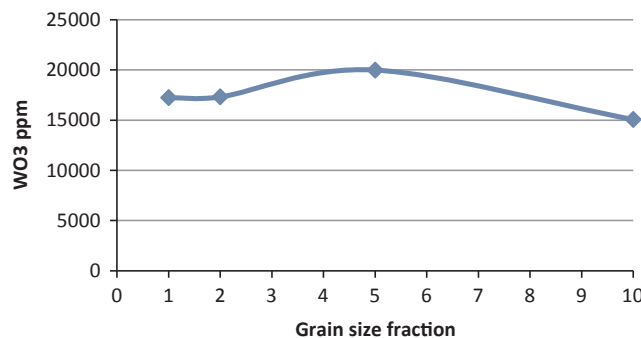


Fig. 8. The WO<sub>3</sub> grade of sinks for the various grain size fractions.

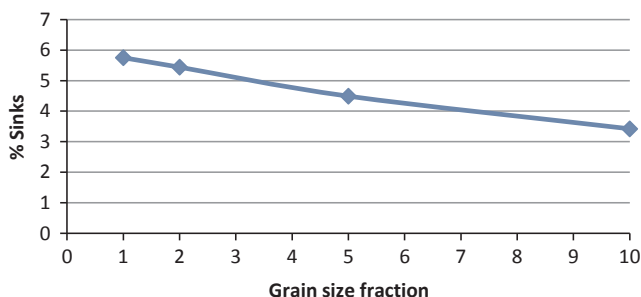


Fig. 7. Diagram illustrates the linear relationship between grain size fraction and weight % sinks produced by means of TBE separation.

**Table 4**  
Concentration of weight% THM/Sinks per grain size fraction.

Sample Nr.	% THM/Sinks
– 10 mm	3.42
– 5 mm	4.49
– 2 mm	5.44
– 1 mm	5.75

**Table 5**  
WO<sub>3</sub> grade of slimes, sinks and floats (from XRF assay).

Sample Nr	Fraction	WO <sub>3</sub> (ppm)
– 10 mm	– 45 μm (slimes)	2495
– 5 mm	– 45 μm (slimes)	2338
– 2 mm	– 45 μm (slimes)	2245
– 1 mm	– 45 μm (slimes)	1896
– 10 mm	Conc./THM (sinks)	15060
– 5 mm	Conc./THM (sinks)	19980
– 2 mm	Conc./THM (sinks)	17310
– 1 mm	Conc./THM (sinks)	17240
– 10 mm	Floats	215
– 5 mm	Floats	449
– 2 mm	Floats	838
– 1 mm	Floats	1039

20 × 20 × 20 mm resulting in 20 μm resolution scans. This is a practical solution which allowed good representative results in reasonable scan times. If larger samples are selected, too many X-ray penetration artefacts are produced and if much smaller sample size is used the results are not considered to be representative. The results revealed that the resolution of the instrumentation did not allow meaningful results for the slimes fraction, as most of the tungsten particles are smaller or close to the resolution selected, resulting in loss of contrast through the partial volume effect. The floats and sinks however, showed a sharp contrast between gangue, other ore minerals and scheelite and revealed

**Table 6**  
Recovery of WO<sub>3</sub> from size fractions with head grade of 0.207%WO<sub>3</sub>.

Sample Nr	Recovery kg/t	%WO <sub>3</sub> recovery
– 10 mm	0.515	24.9
– 5 mm	0.897	43.3
– 2 mm	0.942	45.5
– 1 mm	0.991	47.9

results that are useful indicators of scheelite liberation and beneficiation. In addition the results showed that the TBE separation was efficient with hardly any liberated scheelite reporting to the floats fraction (Figs. 10–13).

The microCT scans also visually demonstrated the grain sizes of scheelite relative to the crushed particle size. This was shown for example in Fig. 10, where the floats of the – 10 mm fraction contain large gangue particles with abundant locked scheelite. The poor scheelite recovery of this sample was attributed to the abundance of grains locked in gangue (Fig. 9). As the sample was crushed to a finer grain size the quantity of scheelite locked in gangue was reduced significantly and recovery improved. Floats of the – 1 mm sample showed a decrease in the abundance of gangue locked scheelite and suggests that additional milling/grinding to a finer grain size e.g. – 0.5 mm will enhance liberation and recovery, but at the cost of increased slimes generated.

Results of the CT scans were also used to determine the WO<sub>3</sub> grade of each fraction by scheelite volume calculations which were converted to mass. The outcome of the various iterations (5 microCT scans of every size fraction for floats and sinks) is presented in Fig. 14. Correlation between measured microCT results and those determined by XRF are promising for the 10 mm and 5 mm fractions for both the floats and sinks. The finer fractions however indicated a consistently poor correlation deteriorating towards the – 1 mm fraction. This is attributed to the possibility that a larger number of scheelite grains are smaller than or close to the scan resolution selected (20 μm) and are not included in the calculation resulting in a lower grade. The poor correlation of the – 1 and – 2 mm fractions could be predicted due to lack of a clear peak in the grey-value histogram during segmentation, indicating that higher resolution is required. The present methodology is consequently not

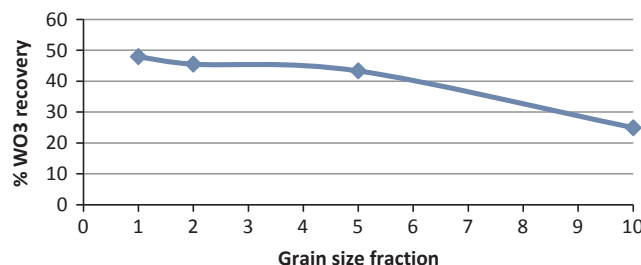
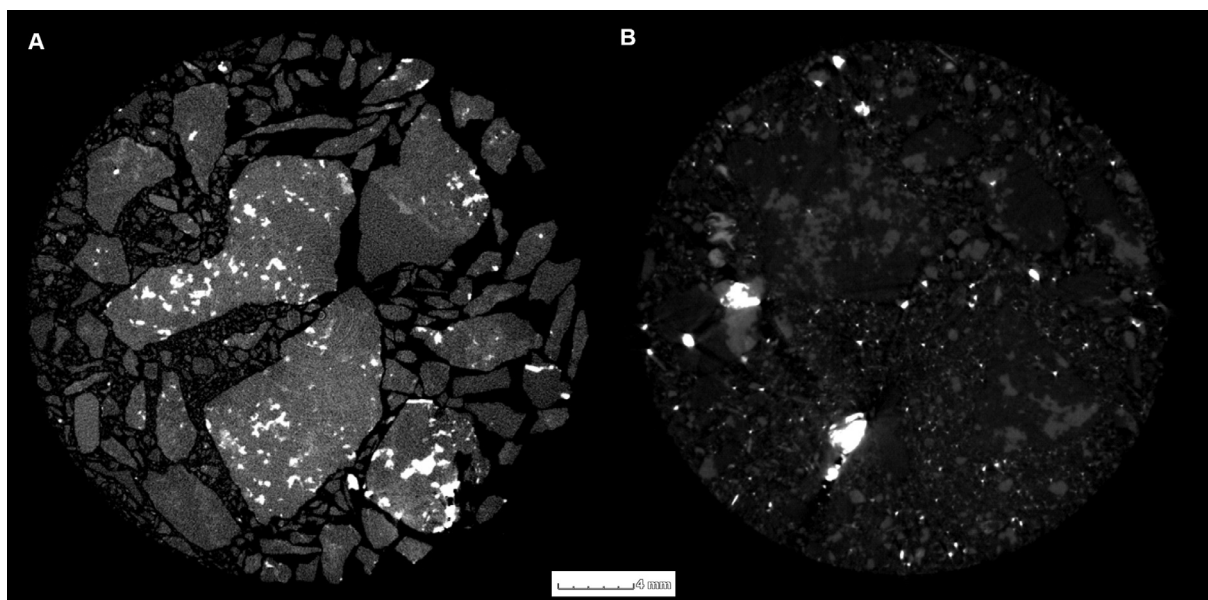


Fig. 9. Graph showing WO<sub>3</sub> recovery as a percentage of the head grade of 0.207% WO<sub>3</sub>.



**Fig. 10.** CT scan of the floats (A) and sinks (B) of the  $-10$  mm size fraction. Liberation of scheelite (bright grains) is poor and most of the fine-grained scheelite ( $0.1$ – $1$  mm) remains locked in the large gangue particles. The sinks show a variation of liberated and locked scheelite. Grains with pyrite and pyrrhotite and disseminated scheelite will also report to the sinks (intermediate grey colours).

effective for the finer scheelite particles and requires refinement such as by selecting smaller sample volumes for analysis that will facilitate higher resolution. To demonstrate this, the  $-2$  mm concentrate (sink) fraction was sampled in a smaller container and analysed at  $5$   $\mu\text{m}$  in a single scan, using an identical methodology. The histogram (Appendix A) shows a clear peak for scheelite and measured scheelite grade was increased by 25% compared to the  $20$   $\mu\text{m}$ , indicating an increase in detected scheelite. The mean grain size also decreased from  $120$   $\mu\text{m}$  to  $60$   $\mu\text{m}$ , indicating that a larger number of smaller grains were positively identified.

The current results at  $20$   $\mu\text{m}$  resolution therefore favours quantitative analysis of the coarser scheelite grains and qualitative visual analysis of finer grains. The method shows promise as an ore grade

indicator as well as providing additional information of mineral associations.

Particle size analyses of scheelite for the various fractions were conducted using the same microCT data. Results of the four size fractions for floats and sinks are shown in Fig. 14. It can be accepted from Figs. 10–13 that all the scheelite grains present in the floats fraction are locked with silicate and minor sulphide gangue. Size of the scheelite grains in the floats are variable particular in the coarser fraction and gradually becomes finer towards the  $-1$  mm fraction. As expected the coarser scheelite has been liberated from gangue by finer grinding. The floats of the  $-1$  mm fraction are dominated by locked  $0.1$ – $0.2$  mm scheelite whereas the liberated grains in the sinks are mostly between  $0.15$  and  $0.2$  mm (Figs. 13 and 15). This suggests that finer grinding to

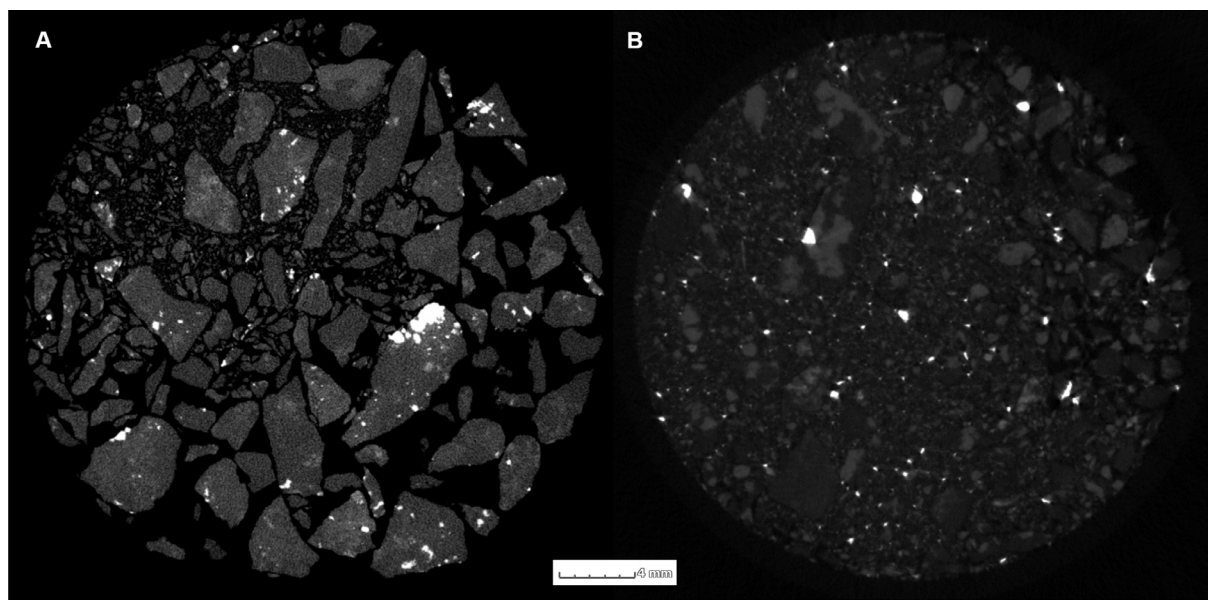


**Fig. 11.** CT scan of the floats (A) and sinks (B) of the  $-5$  mm size fraction. Fine-grained scheelite locked in gangue will report to the floats. Note the absence of free scheelite which indicates that the heavy liquid separation was effective. Sinks are dominated by fine-grained liberated scheelite particles and minor coarse-grained gangue with disseminated scheelite and sulphides.

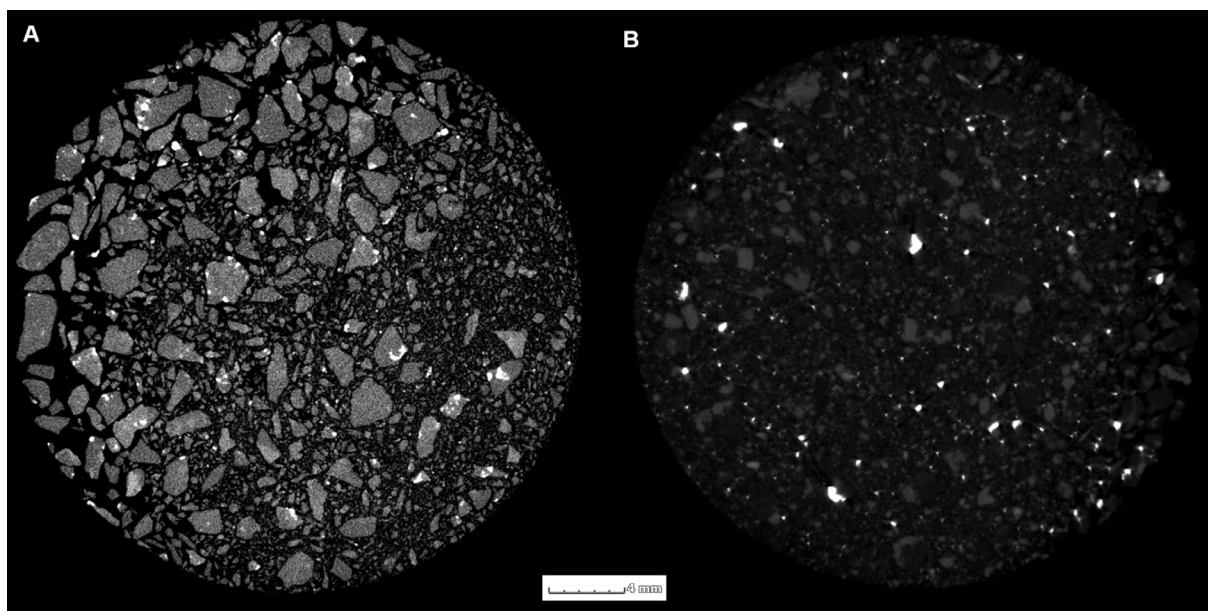


Fig. 12. CT scan of the floats (A) and sinks (B) of the  $-2$  mm size fraction. Further reduction of particle size has increased liberation of scheelite from the larger particles and has improved recovery. Some fine-grained scheelite remained locked in gangue in the sinks.

$0.5$  mm for example has the potential to liberate the locked fractions and contribute towards the overall recovery.

Histograms of the scheelite grain size distribution of the sinks (concentrates) illustrate that the grain size becomes more homogenous towards the  $-1$  mm fraction. It shows a narrow distribution between  $0.15$  mm and  $0.2$  mm with few grains  $> 0.55$  mm (Fig. 15). The dominant grain size for all sink/float fractions however remains between  $0.15$  mm and  $0.25$  mm and indicates that grinding and liberation of scheelite generates a similar size fraction distribution. The coarser grained “tail” of the histogram becomes shorter with the finer e.g.  $-1$  mm fraction (Fig. 15). This indicates that the scheelite concentrate feed (sinks) to the next milling phase will have a narrow grain size

distribution as shown by the  $-1$  mm fraction. This milling phase will further reduce the scheelite grain size a feature that will have to be accommodated if flotation is considered as a beneficiation method.

## 5. Discussion and conclusions

The primary aim of the study was to separate scheelite from the Riviera ore by means of TBE. The results showed that the maximum recovery of  $47.9\%$  was achieved by crushing down to  $-1$  mm grain size. It is anticipated that crushing down to  $-0.5$  mm could increase recovery but not significantly. This result was supported by microCT scanning images which showed that scheelite locked in gangue particles

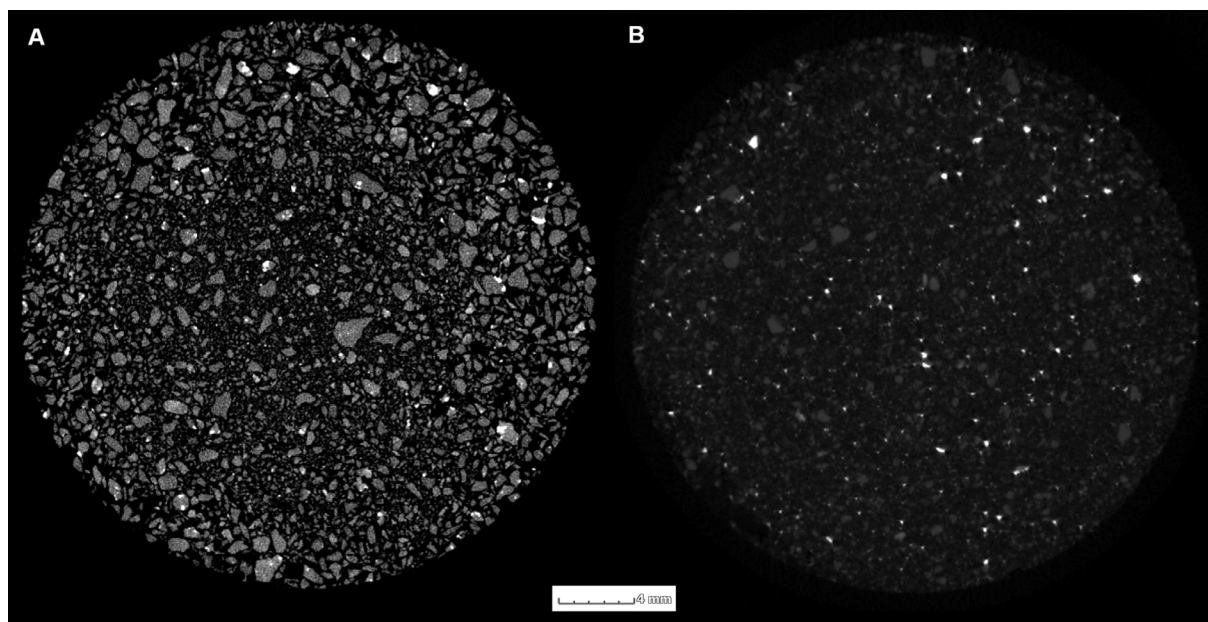


Fig. 13. CT scan of the  $-1$  mm size fraction floats (A) and sinks (B). Scheelite (bright particles) remains locked with gangue minerals (grey) and have not been liberated in the floats. Scheelite particles have a size range between  $0.5$  and  $0.1$  mm. Note the absence of free scheelite which shows that the heavy medium separation was effective. The sinks show abundant liberated scheelite as fine disseminations ( $0.1$ – $1$  mm) and minor grains as lockings with gangue.

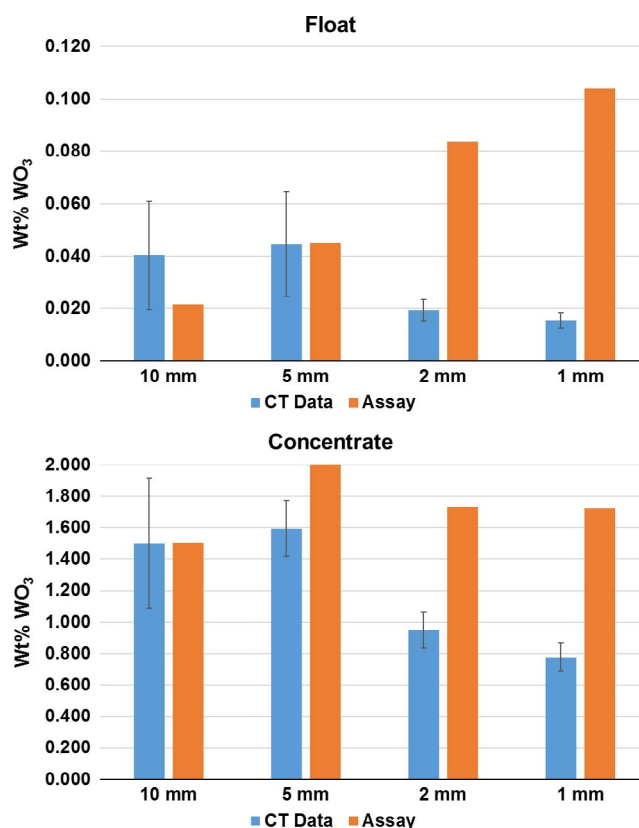


Fig. 14. The correlation of WO<sub>3</sub> grade as determined by microCT scanner at 20 μm and conventional XRF. MicroCT results are averaged over 5 scans of each fraction, hence the error bar. The coarser grain size favours a better quantitative comparison.

was significantly reduced in the –1 mm size fraction. MicroCT scanning images also showed that TBE separation of locked and liberated grains was highly effective. Scheelite present in the floats occurs as fine grains locked with larger gangue particles.

The quantity of slimes generated by the crushing down to –1 mm reached a maximum of 19% and accounts for 17.39% of WO<sub>3</sub> mass loss. The generally high WO<sub>3</sub> grades of the slimes of all four size fractions, is explained by the friable nature of scheelite. It has three cleavage directions also described as planes of weakness, and during blasting and crushing will preferably break along those directions. This will enhance the reduction of scheelite particle grain size compared to the host rock mineralogy which exhibits limited cleavage. Scheelite loss to fines is an aspect that should be addressed in the future and mass loss could be reduced by applying more appropriate crushing techniques and protocols, for example alternatives to disk milling and limitation of over-grinding.

The second and complimentary aim of the study was to use the microCT scanner to provide images of textural features, grain size analyses and to calculate WO<sub>3</sub> grade for the various size fractions. The latter showed promising results for the coarser fractions. The poor correlation of the microCT and XRF results for the fine fraction is attributed to the limited resolution selected for the instrument and abundance of very fine scheelite. This was indicated in the segmentation process by a lack of greyscale peak for scheelite, which can act as a quality indicator for grade determination by microCT. Increased instrument resolution will improve grade calculation to more reliable levels, with the disadvantage of using a smaller sample size (reduced representative sample size and more error-prone sampling possible) and

increasing scan times. In general therefore, when microCT does not produce clear discrimination of the phase of interest, with a separate histogram peak, it will not allow accurate grade determination. This can be overcome in some cases as demonstrated here by higher resolution scanning to better resolve small grains.

Particle size analyses of the various fractions showed that the bulk of the liberated and locked scheelite in the floats is fine-grained. Milling of the floats to allow beneficiation by conventional flotation will reduce scheelite grain size even further and could adversely affect recovery. Beneficiation studies by AAC and partner Union Carbide using conventional flotation during the 1970–1980's, showed a recovery of 61–88% and testifies to the challenge ahead (Woolery, 1981).

Beneficiation of scheelite from a low grade granite hosted resource by means of TBE separation proved disappointing, although the method was efficient. The poor recovery is however a function of excessive slimes generated during milling and overall finely disseminated distribution of scheelite. If WO<sub>3</sub> loss to slimes can be reduced it should be possible to improve recovery to 60% or more for the –1 mm size fraction by TBE separation.

Application of microCT scanning and image analysis to support the present study proved useful and quantitatively contributed towards grade determination, grain size distribution of scheelite and visually towards identification of textural features relating to mineral liberation. The use of this method in assessing the abovementioned minerals processing parameters is promising, particularly when considering the additional information gained from this technique compared to other analytical methods.

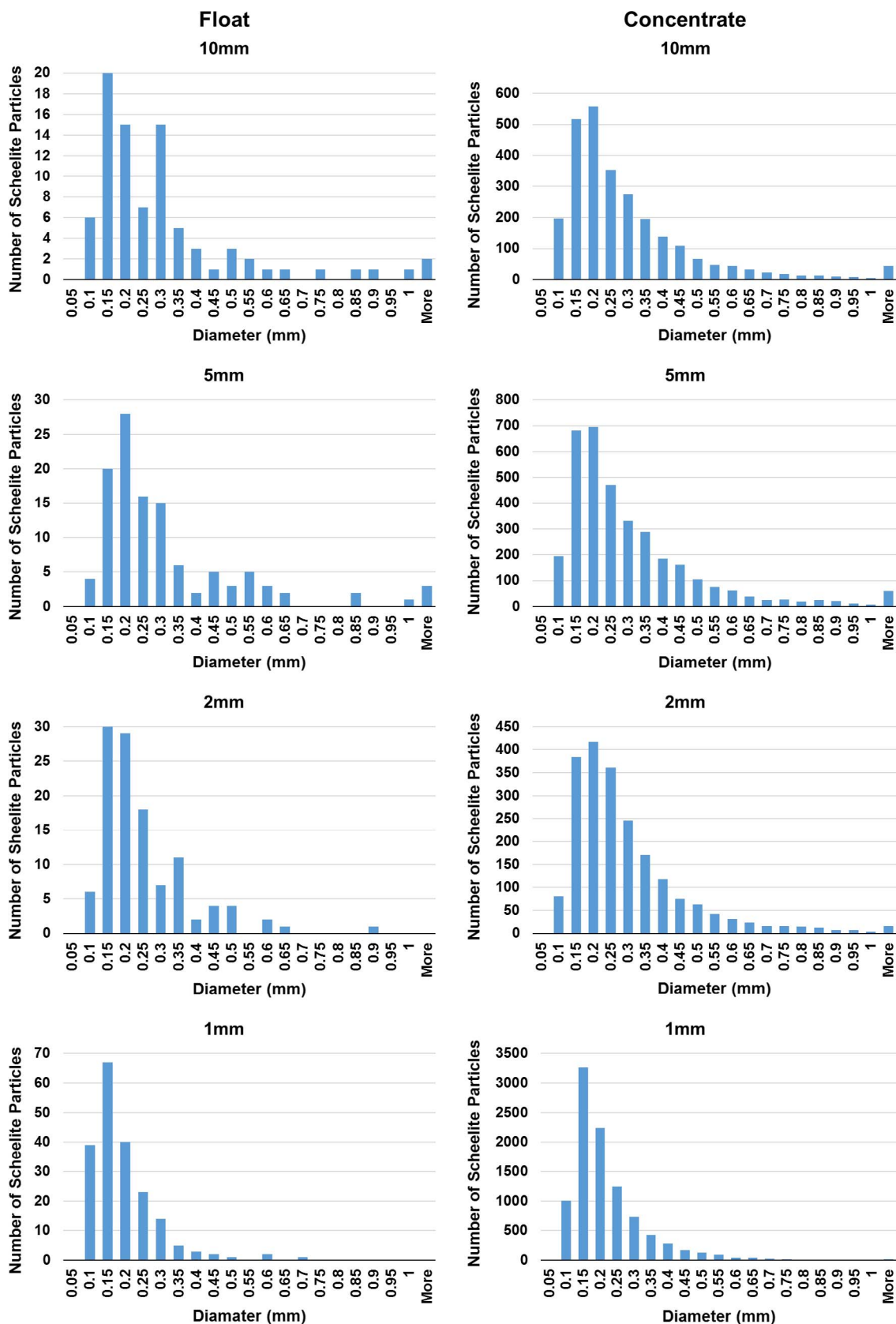
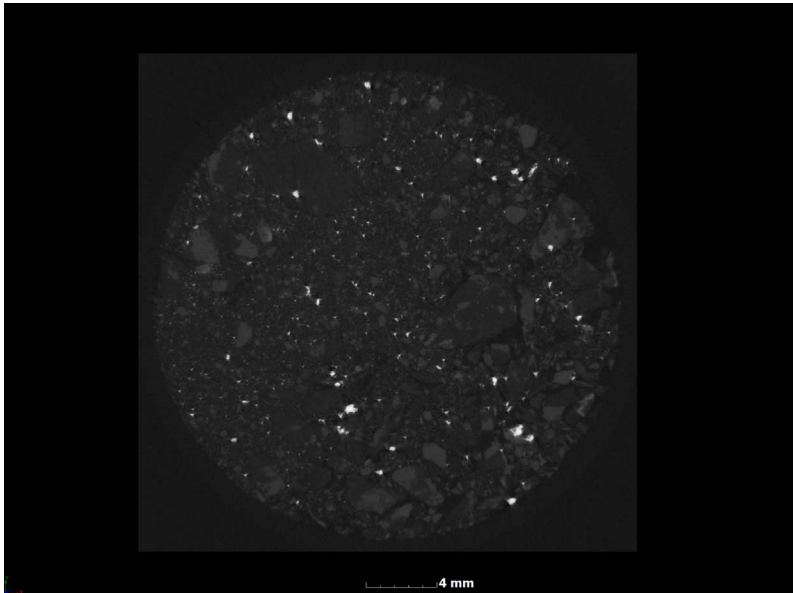


Fig. 15. Histograms showing microCT-calculated grain size distribution of scheelite in floats and sinks of the four grain size fractions.

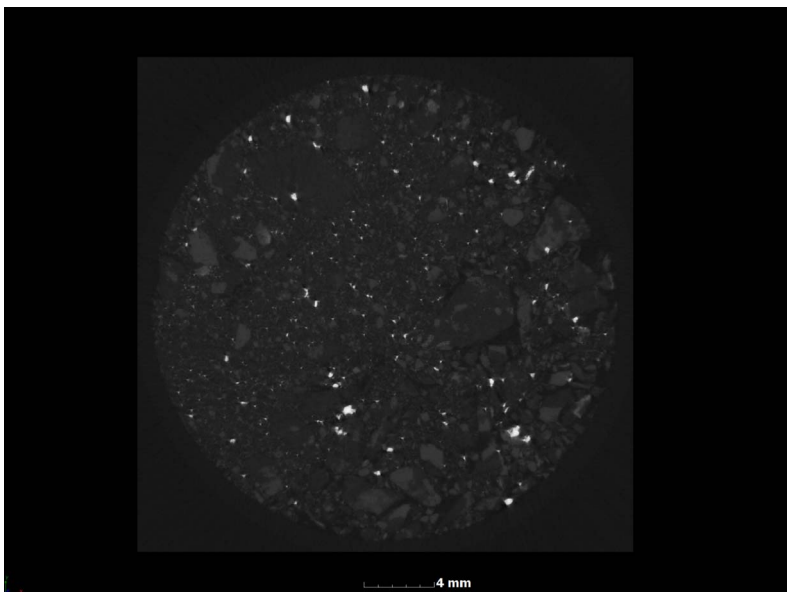
## Appendix A

### Step by step segmentation

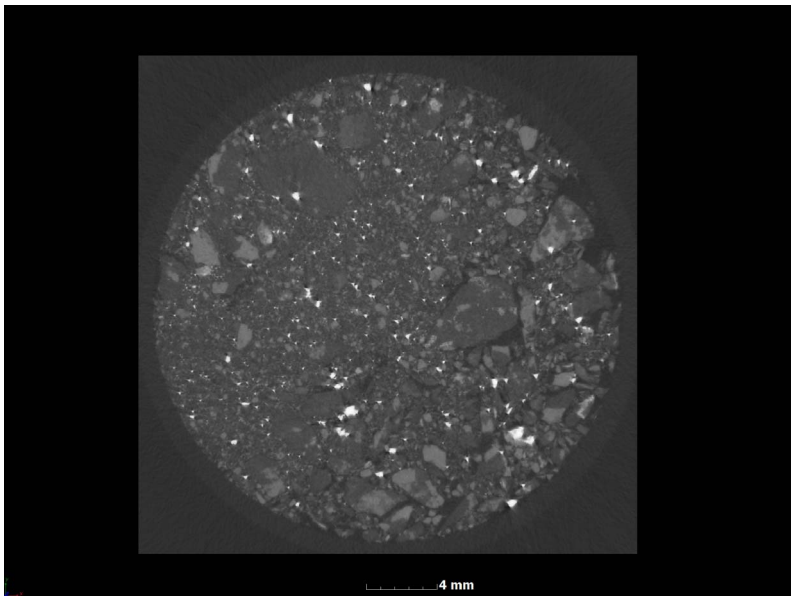
#### Step 1: Raw microCT data



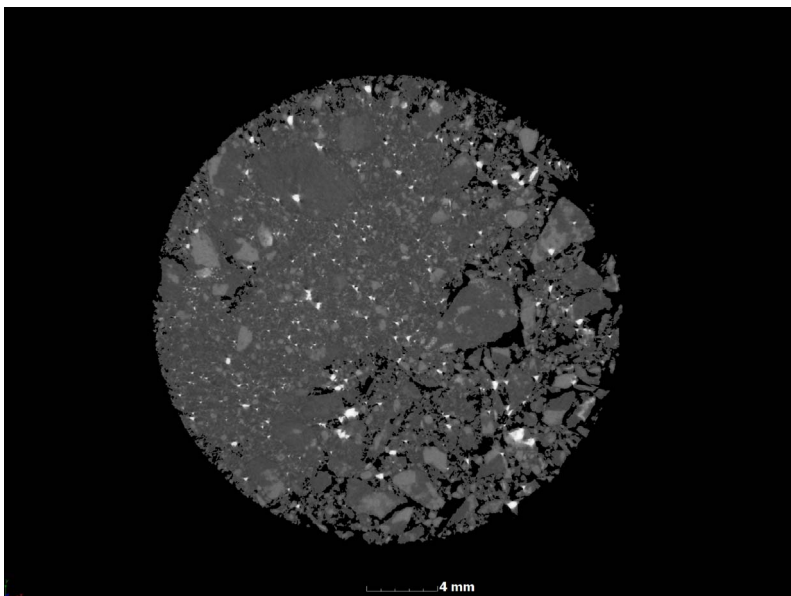
#### Step 2: De-noising – adaptive Gauss filter



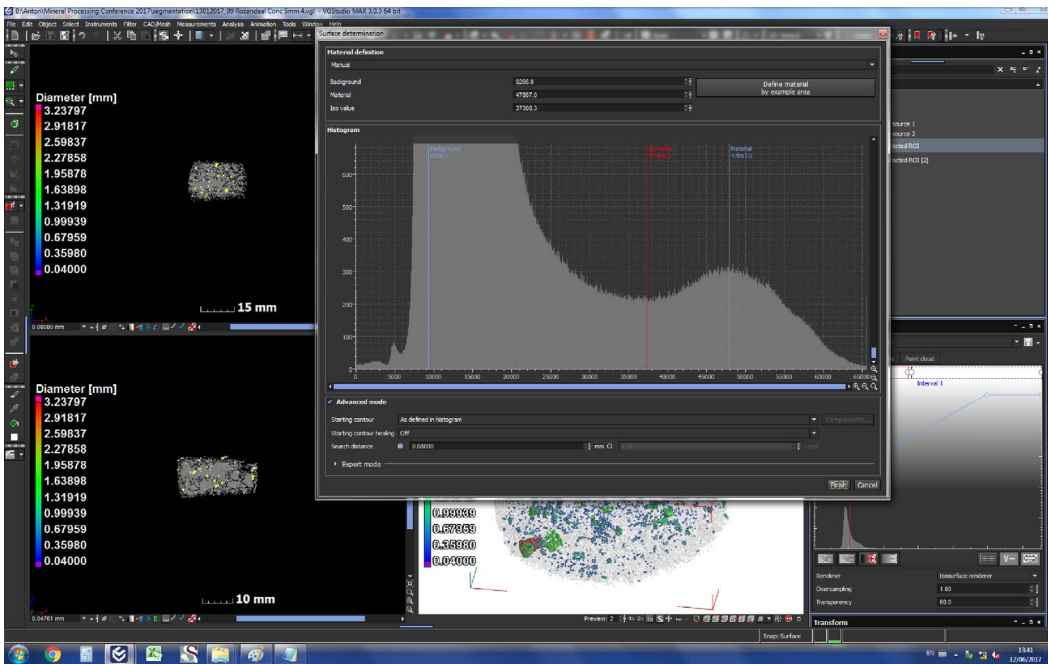
Step 3: Contrasted



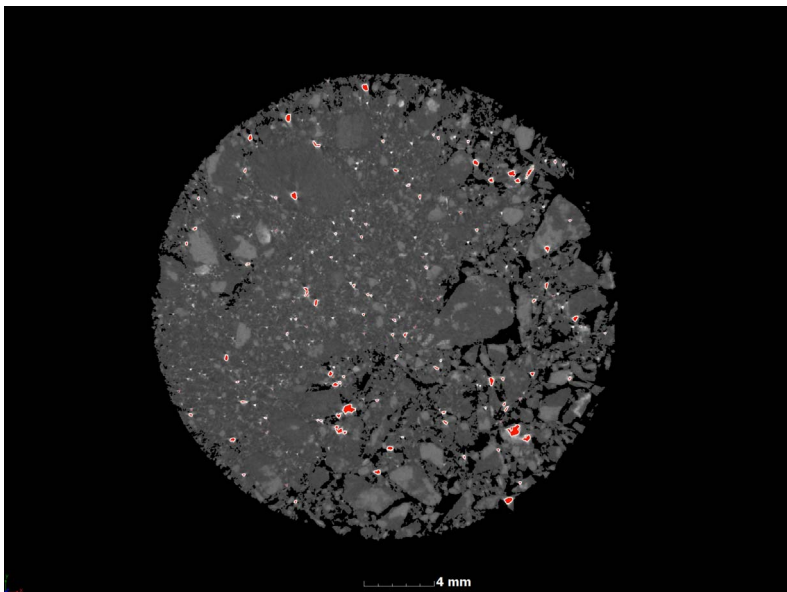
Step 4: Air removal – using region growing tool



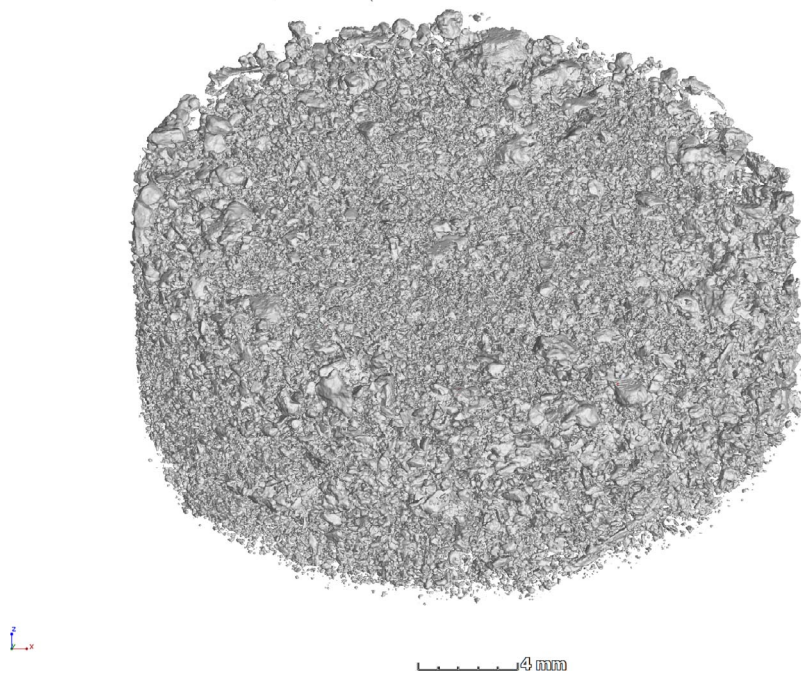
Step 5: Segmentation using lowest position in grey value histogram between peaks, using advanced surface determination function



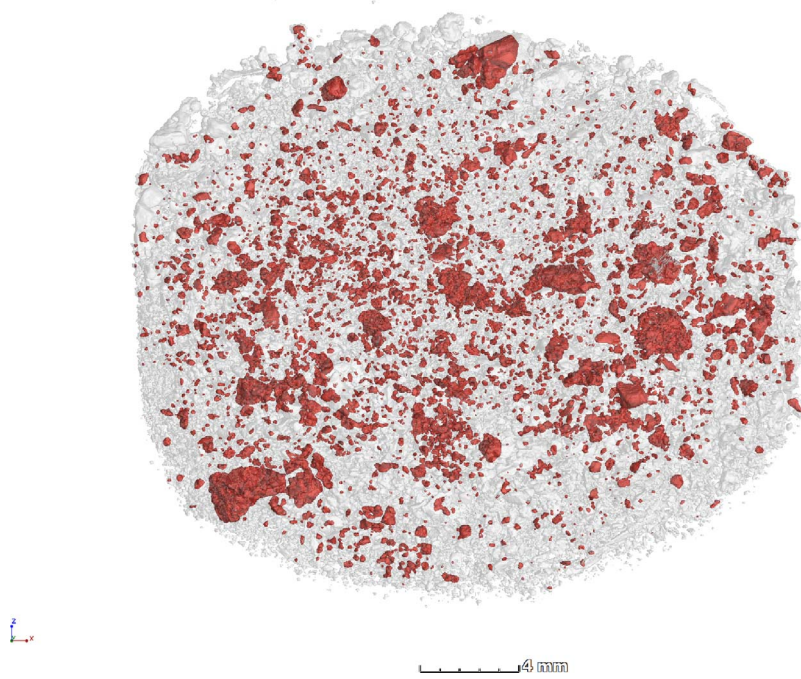
Step 6: Result of segmentation highlighted in pseudo-colour (red) for scheelite



Step 7: 3D image generated from segmentation, first all particles then scheelite

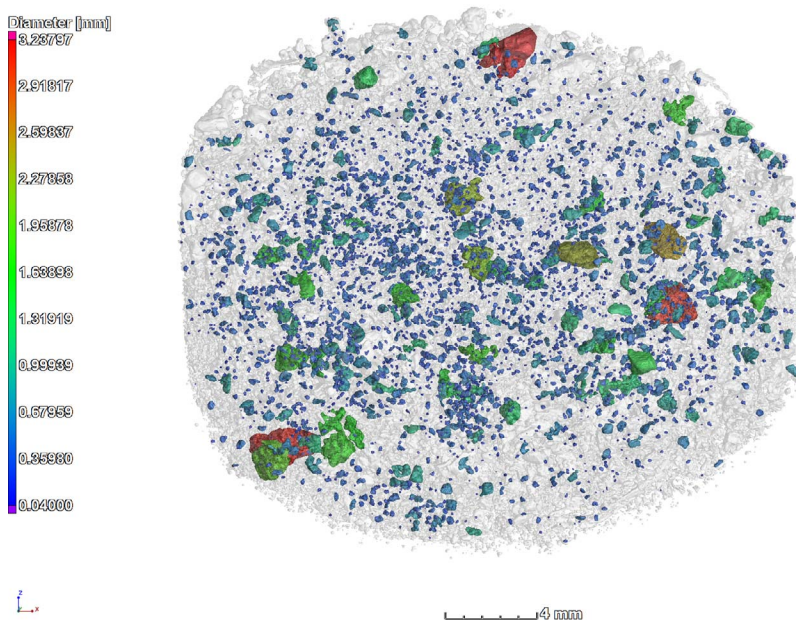


Step 8: Scheelite grain size distribution analysis

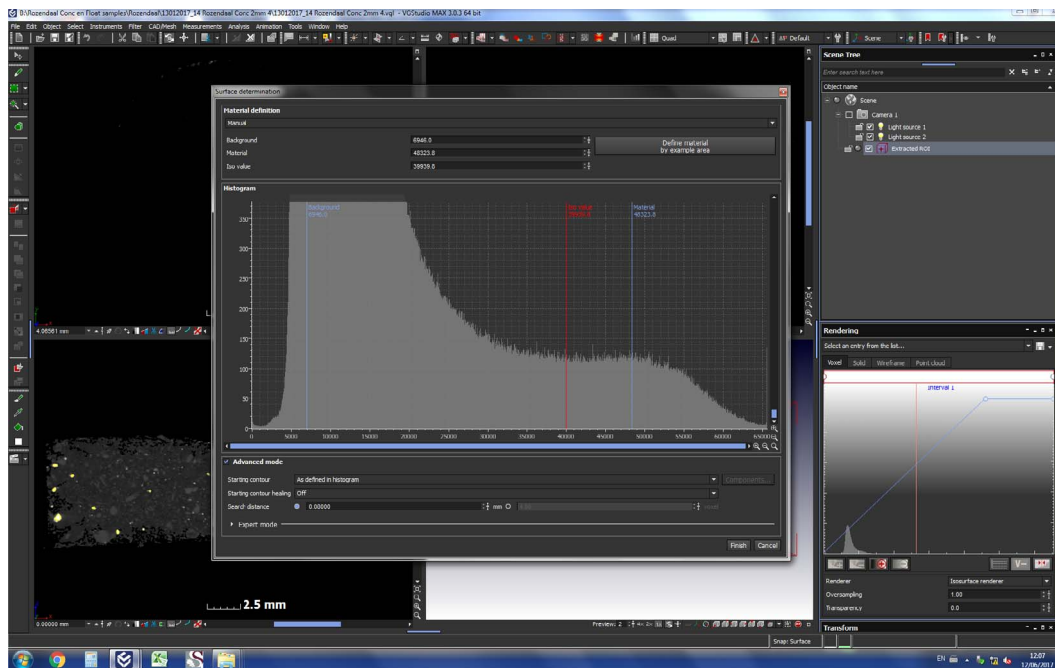


Comparison of segmentation for microCT scans of 2 mm sinks fraction, at 20 μm and 5 μm

At 20 μm, the 2 mm fraction lacks a clear peak for scheelite, due to partial volume effect on small grains relative to scan resolution:



At improved scan resolution on a smaller sample size, the peak is much more clear (5 μm):



## References

- Cnudde, V., Boone, M.N., 2013. High-resolution X-ray computed tomography in geosciences: A review of the current technology and applications. *Earth Sci. Rev.* 123, 1–17.
- Pearce, M.A., Godel, B.M., Fisher, L.A., Schoneveld, L.E., Cleverley, J.S., Oliver, N.H., Nugus, M., 2017. Microscale data to macroscale processes: a review of micro-characterization applied to mineral systems. *Geol. Soc., London, Special Publ.* 453 pp.SP453-3.
- Kyle, J.R., Ketcham, R.A., 2015. Application of high resolution X-ray computed tomography to mineral deposit origin, evaluation, and processing. *Ore Geol. Rev.* 65, 821–839.
- Miller, J.D., Lin, C.L., Hupka, L., Al-Wakeel, M.I., 2009. Liberation-limited grade/recovery curves from X-ray micro CT analysis of feed material for the evaluation of separation efficiency. *Int. J. Miner. Process.* 93 (1), 48–53.
- Du Plessis, A., le Roux, S.G., Guelpa, A., 2016. The CT scanner facility at Stellenbosch University: An open access X-ray computed tomography laboratory. *Nucl. Instrum. Methods Phys. Res., Sect. B* 384, 42–49.
- Du Plessis, A., Broeckhoven, C., Guelpa, A., Le Roux, S.G., 2017. Laboratory X-ray micro-computed tomography: a user guideline for biological samples. *GigaScience* 6 (6), 1–11.
- Le Roux, S.G., Du Plessis, A., Rozendaal, A., 2015. The quantitative analysis of tungsten ore using X-ray microCT: Case study. *Comput. Geosci.* 85, 75–80.
- Rozendaal, A., Theart, H.F.J., 2013. Technical review of the Riviera Tungsten Deposit, Western Cape Province, South Africa. Internal report by SRK consulting for Bongani Minerals Pty (Ltd), pp. 634.
- Pieterse, L., Rozendaal, A., Frei, D., 2014. Mineral chemistry of scheelite as an indicator of hydrothermal fluid evolution of the Riviera W-Mo-REE endoskarn deposit, Western Cape, South Africa. In: IMA Conference, Sandton, South Africa, pp. 205.
- Rozendaal, A., Boshoff, R., 2011. Rare earth element mineralogy and its recovery from the Neoproterozoic Riviera W-Mo deposit, South Africa. In: Proceedings of the 10th International Congress for Applied Mineralogy Trondheim, pp. 605–612.
- Rozendaal, A., Scheepers, R., 1995. Magmatic and related mineral deposits of the Pan-African Saldania belt in the Western Cape Province, South Africa. *J. Afr. Earth Sci.* 21 (1), 107–126.
- Rozendaal, A., Gresse, P.G., Scheepers, R., De Beer, C.H., 1994. Structural setting of the Riviera W-Mo deposit, Western Cape, South Africa. *S. Afr. J. Geol.* 97, 184–195.
- Rozendaal, A., Gresse, P.G., Scheepers, R., Le Roux, J.P., 1999. Neoproterozoic to early Cambrian crustal evolution of the Pan-African Saldania Belt South Africa. *Precamb. Res.* 97, 303–323.
- Walker, P.W.A., 1994. Riviera Tungsten – A discovery case history. *Explor. Mining Geol.* 3 (4), 349–356.
- Woolery, R.G., 1981. Metallurgical Evaluation – Riviera Project. Union Carbide, Metals Division.